

# Outsize Influence of Central American Orography on Global Climate

Jane W. Baldwin<sup>1</sup>, Alyssa R. Atwood<sup>2</sup>, Gabriel A. Vecchi<sup>3,4</sup>, and David S. Battisti<sup>5</sup>

<sup>1</sup>Lamont-Doherty Earth Observatory, Columbia University

<sup>2</sup>Department of Earth, Ocean, and Atmospheric Science, Florida State University

<sup>3</sup>Department of Geosciences, Princeton University

<sup>4</sup>High Meadows Environmental Institute, Princeton University

<sup>5</sup>Department of Atmospheric Sciences, University of Washington

## Key Points:

- Central American orography blocks easterlies and warms SSTs in the northern tropical East Pacific, shaping precipitation and ENSO.
- Low biases in these mountains' height in climate models are partially responsible for pervasive tropical climate simulation biases.
- These and other model biases are improved by alternative interpolation of topography onto model grids to better retain mountain height.

---

Corresponding author: Jane W. Baldwin, [jbaldwin@ldeo.columbia.edu](mailto:jbaldwin@ldeo.columbia.edu)

## Abstract

Global Climate Models (GCMs) exhibit substantial biases in their simulation of tropical climate. One particularly problematic bias exists in GCMs' simulation of the tropical rainband known as the Intertropical Convergence Zone (ITCZ). Much of the precipitation on Earth falls within the ITCZ, which plays a key role in setting Earth's temperature by affecting global energy transports, and partially dictates dynamics of the largest interannual mode of climate variability: the El Niño-Southern Oscillation (ENSO). Most GCMs fail to simulate the mean state of the ITCZ correctly, often exhibiting a "double ITCZ bias", with rainbands both north and south rather than just north of the equator. These tropical mean state biases limit confidence in climate models' simulation of projected future and paleoclimate states, and reduce the utility of these models for understanding present climate dynamics. Adjusting GCM parameterizations of cloud processes and atmospheric convection can reduce tropical biases, as can artificially correcting sea surface temperatures (SSTs) through modifications to air-sea fluxes (i.e. "flux adjustment"). Here we argue that a significant portion of these rainfall and circulation biases are rooted in orographic height being biased low due to assumptions made in fitting observed orography onto GCM grids. We demonstrate that making different, and physically defensible, assumptions that raise the orographic height significantly improves model simulation of climatological features such as the ITCZ and North American rainfall as well as the simulation of ENSO. These findings suggest a simple, physically-based, and computationally inexpensive method that can improve climate models and projections of future climate.

## Plain Language Summary

The Sierra Madre mountain range stretches north to south in Central America. These narrow mountains are important for climate due to their location. They block tropical winds that flow east to west, making winds slower and sea surface temperatures warmer in the tropical East Pacific. This affects tropical rainbands and a pattern of year-to-year climate variability in the tropical Pacific Ocean, called the El Niño-Southern Oscillation, which has impacts across the entire globe. Climate models break the earth up into grid boxes to simulate atmosphere and ocean circulations. Since mountain peaks are smaller than these grid boxes, mountains in climate models, including the Sierra Madre, are shorter than in reality. The low bias in these mountains makes the simulation of climate in the tropical East Pacific different than that observed on earth. We show that these differences can be resolved by making mountains in climate models as high as in reality. Making mountains higher in climate models is also helpful in other places, including North America where the Rockies have a big impact on the atmosphere. Resolving these mountain-related biases can help improve climate models, and our confidence in their simulation of future changes such as global warming.

## 1 Introduction

It is standard practice in GCMs for observed orography to be averaged onto the model grid. For example, in a  $50 \times 50$  km atmosphere/land resolution GCM (e.g. the GFDL CM2.5 Forecast-Oriented Low Ocean Resolution GCM, hereafter FLOR), the orographic height in a given gridcell is based on the value of the observed height spatially averaged over the relevant  $50 \times 50$  km area (see Section 2). This averaging process acts to maintain the mean height of the surface, but smooths out orographic peaks, making mountains "seen" by the GCM atmosphere shorter and less sharp than in reality. This smoothing is further exacerbated in lower resolution GCMs, including those that have been deployed in the most recent Intergovernmental Panel on Climate Change assessments (e.g. the Community Earth System Model version 1.0.5, hereafter CESM,  $0.9^\circ \times 1.25^\circ$  atmosphere/land resolution).

A dominant way orography impacts large-scale climate is by blocking atmospheric flows (Molnar et al., 2010), deflecting winds horizontally or vertically depending on the height of the orographic feature and the atmospheric stratification (Hoskins & Karoly, 1981; Valdes & Hoskins, 1991; White et al., 2017). Vertical deflection also steers the large-scale winds through vortex stretching (Holton, 1973). Recent studies have highlighted that even thin but high orographic features can exert mechanical impacts highly influential for diverse climatic features. For example, the Himalayas form a high wall that blocks cold and dry extra-tropical air from reaching the tropics, and it has been argued that this effect is more important in driving the Indian monsoon than influences of the larger Tibetan Plateau (Boos & Kuang, 2010). Mechanical blocking of wind is also an important component of the northern Tibetan Plateau’s influence on the East Asian Summer Monsoon (Chiang et al., 2015; Kong & Chiang, 2020), the Yunnan-Guizhou Plateau’s influence on the Indian monsoon (Shi et al., 2016), and the Mongolian Plateau’s influence on stationary wave patterns (White et al., 2017).

Outside of Asia, mechanical influences of Central American orography have been shown to influence sea surface temperatures in the northeastern Pacific (Kessler, 2006). The tropical easterlies in the Atlantic are generally blocked by the Sierra Madre, which is a major mountain range that runs northwest-to-southeast across Mexico and extends southward over Central America (Fig. 1a-b). Three lower elevation orographic gaps in the Sierra Madre (from north to south: the Tehuantepec, the Papagayo, and the Panama; Fig. 1a,b) give rise to local wind jets in the tropical East Pacific which in turn drive cool SSTs through increased air-sea heat fluxes and Ekman pumping (Steenburgh et al., 1998; S.-P. Xie et al., 2005; Sun & Yu, 2006; Fu et al., 2017).

The importance of mechanical impacts of mountains across the globe suggests that the smoothing of orography in GCMs might be a significant source of model bias. To test this hypothesis, we make an alternative assumption in regridding observed orography to the GCM grid: in each  $50 \times 50$  km FLOR gridcell we select the highest point from a  $5 \times 5$  minute resolution observed orographic dataset, and choose that to be the height of the relevant gridcell (see Section 2). Compared to the standard averaging practice, this represents a rather extreme alternate assumption. It has the advantage of better capturing peak mountain height in the model, but creates broad regions at higher elevation than in reality (Fig. 1b). The weather modeling community has explored alternative orographic interpolation schemes similar to this, i.e. envelope orography (Wallace et al., 1983; Jarraud et al., 1986), but such methods are not common in atmosphere-ocean coupled climate modeling.

To test the effect of this alternate high orography on climate we run three simulations with GFDL CM2.5-FLOR: 1) a control simulation with standard present day orography (“FLOR Control”; Fig. 1c, Fig. S1b), a simulation where this high orography modification is implemented everywhere on land (“FLOR HiTopo”; Fig. S1c), and another simulation where this modification is only done over Central America (“FLOR CAM”; Fig. 1d). We also run additional simulations with the lower resolution CESM 1.0.5: a control with standard orography (“CESM Control”; Fig. 1f), and a simulation with idealized elevated orography over Central America (“CESM Ideal CAM”; Fig. 1g) (Atwood et al., 2020). The CAM simulations are completed to test the hypothesis that the Central American orography has an outsize influence on climate and that low biases in orography over Central America are particularly influential in biasing the simulated tropical Pacific climatology.

## 2 Methods

The simulations, datasets, and analysis methods used in this study are described below.

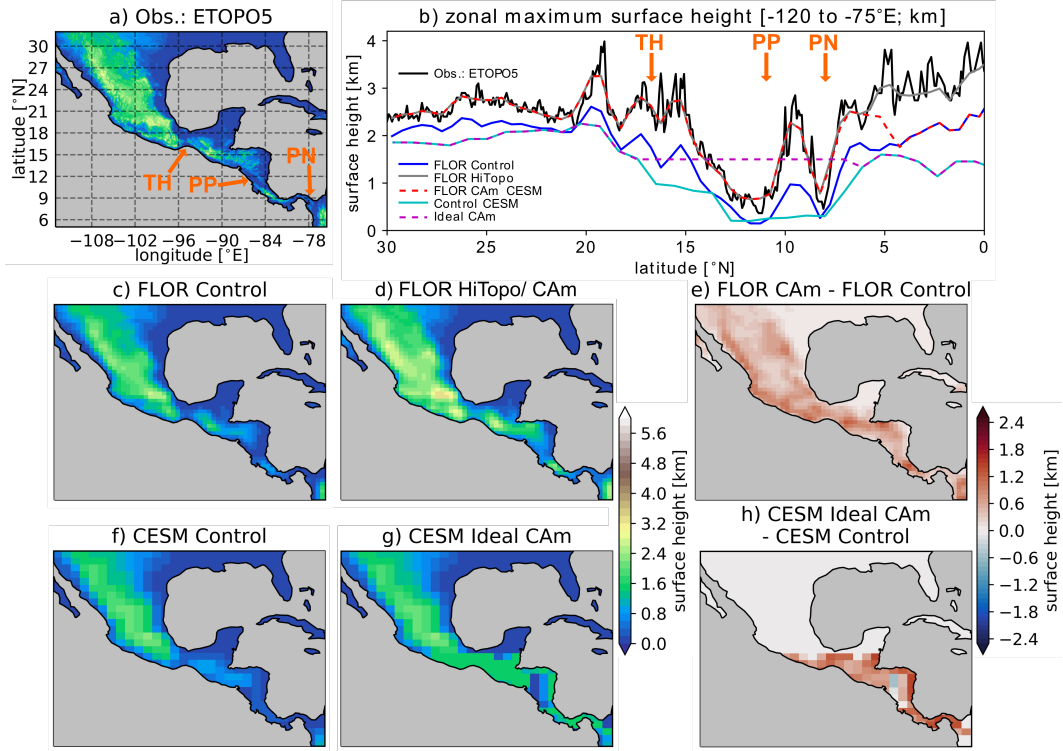


**Figure 1.** Surface height across Central America in observations compared to the boundary conditions in FLOR and CESM. Surface height over Central America is shown from the ETOPO5 5' observed topography dataset (a), and for the FLOR Control (c), FLOR CAM (d), CESM Control (f), and CESM Ideal CAM (g) simulations. Differences in surface height are shown for FLOR CAM and FLOR Control (e) and the CESM Ideal CAM and CESM Control simulations (h). The zonal maximum surface height across Central America (b) is also shown for the observations (black) and each model run– FLOR Control (blue), FLOR HiTopo (grey), FLOR CAM (dashed red), CESM Control (cyan), and CESM Ideal CAM (dashed magenta). Where different boundary conditions are the same appears as multi-colored due to layering of dashed and solid lines. Note that FLOR HiTopo and FLOR CAM boundary conditions are identical within Central America, but in other locations FLOR CAM follows the FLOR Control surface height while FLOR HiTopo is further elevated (see Section 2). In (a) and (b), the locations of the Central American low-elevation gaps are designated with orange arrows and lettering (TH for Tehuantepec, PP for Papagayo, and PN for Panama).

## 2.1 GCM Simulations

Two GCMs are used in this study– CESM 1.0.5 and CM2.5-FLOR. Both are fully atmosphere-ocean coupled models. CESM 1.0.5 was developed at the National Center for Atmospheric Research, and has horizontal resolutions of  $0.9 \times 1.25^\circ$  in the atmosphere/land and nominal  $1 \times 1^\circ$  in the ocean (uniform  $1.1^\circ$  in longitude, variable in latitude from  $0.27^\circ$  at the equator to  $0.54^\circ$  at  $33^\circ$  latitude). CM2.5-FLOR (hereafter “FLOR”) was developed at NOAA’s Geophysical Fluid Dynamics Laboratory, and features a rather high resolution approximately  $50 \times 50$  km atmosphere/land using a cubed-sphere finite volume dynamical core (Putman & Lin, 2007), and a relatively lower resolution  $1 \times 1^\circ$  ocean (telescoping to  $0.333^\circ$  meridional spacing near the equator). FLOR, which stands for “Forecast-oriented Low Ocean Resolution”, has been shown to have improved skill

in simulating precipitation climatology, extreme heat and rainfall events, and seasonal forecasting compared to lower resolution models comparable to CESM 1.0.5 (Jia et al., 2014, 2016; Krishnamurthy et al., 2018; van der Wiel et al., 2016).

Orographic boundary conditions play a few different roles in GCMs, controlling surface height that the resolved atmospheric circulation interacts with, and parameterizations for sub-gridscale processes including gravity wave drag, boundary layer roughness, and aspects of the land model such as vegetation type and river flow. The focus of this study is on mechanical influences of orography on atmospheric circulation, so we alter just the boundary condition controlling surface height. Gravity wave drag and boundary layer roughness depend on parameterizations based on subgridscale variance of topography, which is kept identical in the Control and modified orography experiments. Static rather than dynamic vegetation is used, such that the vegetation type does not respond to the orographic alterations.

We run Control simulations of each GCM (“FLOR Control” and “CESM Control”), in which radiative forcing is kept constant at pre-industrial levels (1860 in FLOR, 1850 in CESM), and standard orography is used. In these experiments, which reflect typical GCM treatment of orography, the orographic height in a given gridcell is the area-average of observed height in that gridcell.

We also run a few different perturbation experiments with non-standard orography but retaining pre-industrial radiative forcing. With FLOR, we instead set orography in each gridcell to be the maximum observed height across the relevant gridcell, an experiment we refer to as “FLOR HiTopo”. The observed orography used is the ETOPO5  $5\times 5'$  resolution dataset available from NOAA’s National Center for Environmental Information. This type of alternative topographic interpolation was also performed over a limited area in a recent study that focuses on the effects of the Andes (Xu, 2019). To isolate the effect of Central American orography, we run an additional experiment in which orography is elevated only over Central America (“FLOR CAM”), specifically over two adjacent regions 14 to 32°N, -113 to -85°E, and 5 to 14°N, -95 to -75.5°E. Note that the resultant FLOR HiTopo and FLOR CAM surface height while much higher than that of FLOR Control is slightly lower than observed mountain peak height (Fig. 1b), due to regridding from the regular lat-lon of the topography data to the GCM cubed-sphere grid.

The FLOR simulations begin with a “cold start”, in which temperature and other values start out as constant throughout the atmosphere, and then dynamically spin up over the first few time steps. We found a “cold start” allowed the GCM to more robustly adjust to different orographic boundary conditions compared to providing atmospheric initial conditions from a preexisting simulation. We run each simulation for 200 years, analyzing years 31 to 200 to allow for model spin-up.

In CESM 1.0.5 the height of the mountains across Central America were raised to 1500 m (between 7-18°N, 120-76°W; Fig. S1) (Atwood et al., 2020). Because the intent of this (earlier) orography modification was simply to reduce the tropical SST and low-level wind biases in the eastern Pacific associated with poor resolution of Central American orography, rather than improve the representation of Central American orography, we refer to this simulation as “CESM Ideal CAM”. This simulation was branched from year 863 of the 1300-year-long pre-industrial CESM Control simulation, then run for 300 years. For CESM Control years 1201-1300 are analyzed, whereas for CESM Ideal CAM all 300 years simulated are analyzed.

## 2.2 Observed Datasets

A variety of observed climate datasets are used to compare to the model simulations and evaluate biases. We use zonal and meridional wind and surface wind stress data

from the Modern-Era Retrospective analysis for Research and Applications, Version 2 (MERRA-2;  $0.5^\circ \times 0.625^\circ$ ; 1/1980-1/2020; Gelaro et al. (2017)). We use SSTs from the Hadley Centre Global Sea Ice and Sea Surface Temperature dataset version 1.1 (HadISST;  $1^\circ \times 1^\circ$ ; 1/1871-1/2020; Rayner et al. (2003)). For ocean surface currents we use the Ocean Surface Current Analysis Real-time data at 15 meters depth (OSCAR;  $0.33^\circ \times 0.33^\circ$ ; Bonjean and Lagerloef (2002)). Finally, we use three different precipitation datasets: the Integrated Multi-satellite Retrievals for GPM (IMERG;  $10 \text{ km} / 0.1^\circ$ ; 6/2000-7/2019; Huffman et al. (n.d.)), the CPC Merged Analysis of Precipitation (CMAP;  $2.5^\circ \times 2.5^\circ$ ; 1/1979-9/2019, P. Xie and Arkin (1997)), and the Global Precipitation Climatology Project monthly precipitation dataset version 2.3 (GPCP;  $2.5^\circ \times 2.5^\circ$ ; 1/1979-8/2018; Adler et al. (2003)).

### 2.3 ENSO Metrics

In assessing the fidelity of ENSO simulation, SST anomalies are calculated by averaging over the Niño 3 and Niño 3.4 regions (respectively,  $-5$  to  $5^\circ\text{N}$ ,  $-150$  to  $-90^\circ\text{E}$ , and  $-5$  to  $5^\circ\text{N}$ ,  $-170$  to  $-120^\circ\text{E}$ ), and then removing the seasonal cycle. These raw SST anomalies are used to determine the ENSO variance by month, whereas three-month running means of the SST anomalies are used for calculating the ENSO power spectra.

## 3 Results

Consistent with previous work, we find large biases in the GCMs' simulation of eastern Pacific climate. In Central America, the southern extension of the Sierra Madre is known to block the flow of tropical easterly winds except in the few lower-elevation gaps in the mountains. In many GCMs, including FLOR and CESM 1.0.5, low-level trade winds in the East Pacific proximal to these mountains are biased too strong (Song & Zhang, 2020) (Fig. 2a,c), leading to negative SST biases in this region (Fig. 2b,d). The negative SST bias is most pronounced where observed topography is high between the Tehuantepec and Papagayo gaps, and between the Papagayo and Panama gaps. North and south of this cold bias, there are also positive SST biases, which are adjacent to the Baja California Peninsula and along the western coast of South America, respectively. In the lower-resolution CESM Control the cold bias west of Central America and the warm biases to the south and especially north of it (off the coast of Baja) are generally stronger and broader than in the FLOR Control.

The raised orography in FLOR HiTopo leads to reduced biases in near-surface winds and SSTs, especially in the tropical East Pacific and to some degree in the western tropical Atlantic and Gulf of Mexico (Fig. 2a-b,e-f). These wind and SST bias reductions are also seen in FLOR CAM and CESM Ideal CAM, indicating that the elevated Central American orography is responsible for these improvements (Fig. 2g-h,i-j). In all three simulations with altered orography, raised Central American mountains increase blocking of tropical easterlies, reducing wind speed over the northern tropical East Pacific. This decreased wind speed in turn leads to warmer SSTs through a combination of reduced latent and sensible heat fluxes from the ocean surface, and reduced upwelling and entrainment of deeper cold waters. To the west of Central and South America, these changes in the surface winds and SSTs substantially decrease the model biases compared to observations, with the strongest effects during MAM when the Pacific ITCZ is at its southernmost position and the trade winds north of the equator in the tropical East Pacific are correspondingly strong and northeasterly (compare Fig. 2 and Fig. S2; effects in DJF and JJA are intermediate to MAM and SON).

To the north and south of this region of warming in FLOR HiTopo and FLOR CAM, and to the north in CESM Ideal CAM, the raised orography results in cooler surface waters, some of which further reduce the SST biases in these regions (Fig. 2f,h,j). The cooling to the north near the Baja Peninsula is coincident with enhanced wind speeds likely caused by convergence and upward motion to the south, over the region of warmer SSTs



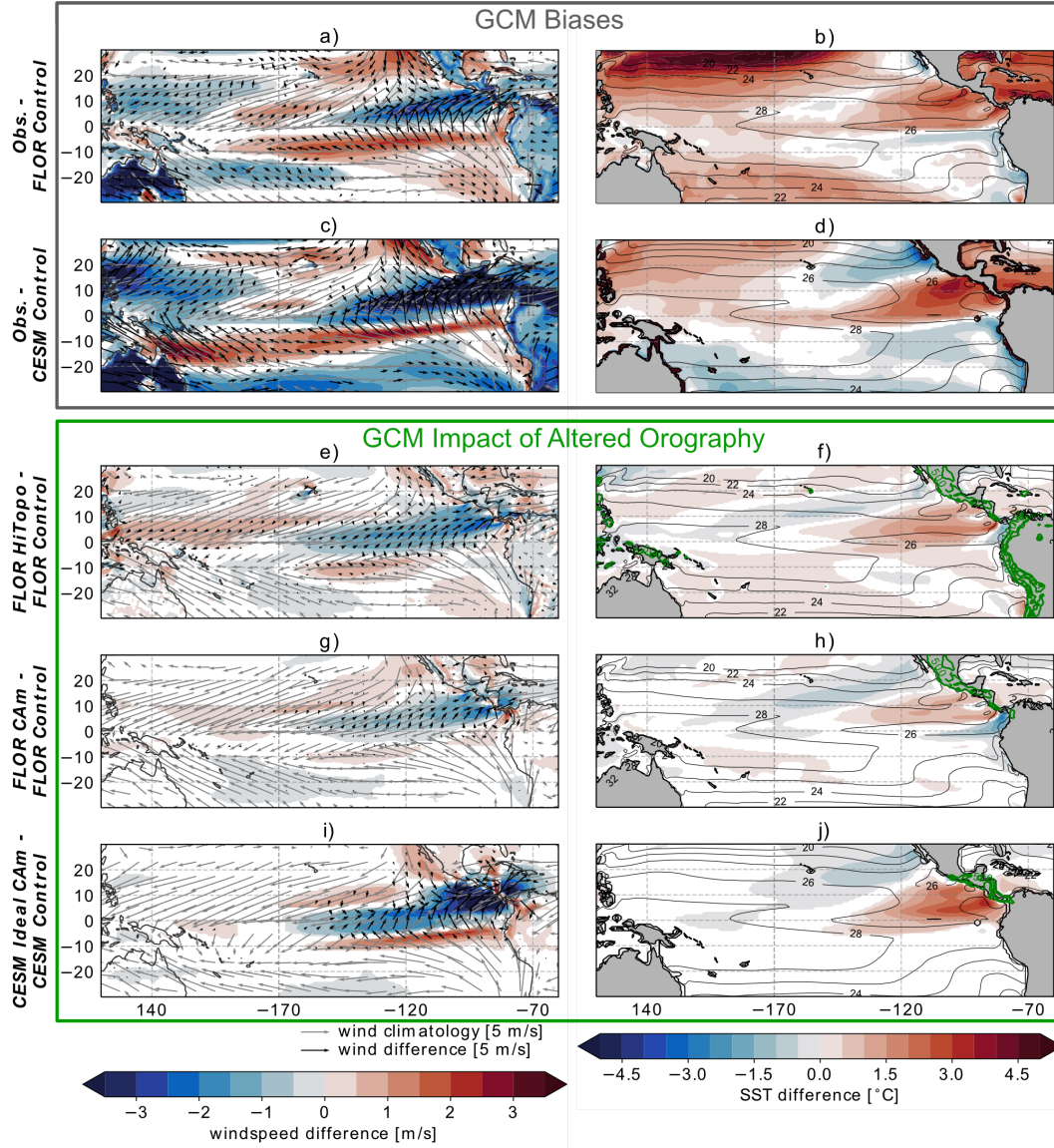


**Figure 2. Influence of orography on tropical Pacific winds and SSTs for March-May (MAM).** MAM average wind vectors and speeds are shown in the left column (a,c,e,g,i), with windspeed differences shaded, wind differences in black vectors, and the relevant Control wind climatology in grey vectors. Wind data is taken from the lowest atmospheric level available in the 3-D data ( $\sim 950$  hPa) from the MERRA-2 reanalysis (Obs.), FLOR output, or CESM output. MAM average SSTs are shown in the right column (b,d,f,h,j) with SST differences shaded, and relevant Control climatology in black contours. The observed SST data is HadISST. In the lower right-column panels (f,h,j) the difference in the surface height boundary conditions between the relevant perturbation simulations and Control simulations is contoured in green. In all panels, differences that are not significant at a 90% level based on a two-sided  $t$ -test are masked out (i.e. are white for the filled contours, and do not appear for the vectors).

adjacent to Central America. In FLOR HiTopo and FLOR CAM, cooling to the south originates directly outside of the Panama gap and stretches into the Pacific, suggesting

that it results from enhanced wind flow through the gap due to elevated Central American orography; the fact that CESM Ideal CAM does not have a Panama Gap and exhibits no cold anomaly in this region further supports this interpretation (Fig. 1h and 2j). In contrast, a warm bias occurs in the region south of the equator in the eastern Pacific in the FLOR Control and CESM Control, which does not exhibit a clear connection to the Panama gap (Fig. 2b,d).

In summary, the strong cool bias west of Central America and extending about 6000 km into the tropical Pacific is clearly tied to orographic biases in Central America, as is some of the warm bias adjacent to the Baja California Peninsula. In contrast, the warm bias west of South America is not improved in these experiments, and may be associated with low-cloud biases not explored in this work.

In addition to impacting surface heat fluxes, altered orography over Central America also influences SSTs through its effects on oceanic circulation. The North Equatorial Counter Current (NECC) flows eastward at about 5-10°N in the Pacific (Fig. 3a). It is weak and zonally truncated in the FLOR Control, but spans the Pacific with similar magnitude to observations in FLOR HiTopo and FLOR CAM (Fig. 3b-e). CESM Ideal CAM also exhibits a more realistic magnitude NECC than CESM Control, though the improvement is less dramatic than in the FLOR simulations (Fig. S3). Sverdrup theory describes the NECC as arising from the meridional gradient in wind stress curl (Sverdrup, 1947; Reid, 1948), and these changes between simulations are consistent with changes in the wind stress curl. While in the FLOR Control the meridional gradient of wind stress curl proximal to the NECC is biased low, elevated orography alters this gradient to be closer to observations both in magnitude and position of the peak (Fig. 3f). The NECC carries warm water from the west Pacific warm pool to the cooler tropical northeastern Pacific. In turn, in both FLOR HiTopo and FLOR CAM, the tropical northeastern Pacific SSTs are warmed by both the weakened local wind speeds and the strengthened NECC.

Biases in the simulation of tropical precipitation are partly driven by SST biases (Oueslati & Bellon, 2015). Thus, the improvements in simulation of winds and SSTs west of Central America in the raised orography simulations should result in more realistic precipitation in the eastern Pacific. Indeed, compared to the Control simulations, in FLOR HiTopo, FLOR CAM, and CESM Ideal CAM, precipitation increases greatly in the northeastern tropical Pacific and decreases slightly in the southern branch of the ITCZ (Fig. 4), effectively shifting the eastern Pacific ITCZ northward (Fig. 5). These effects are strongest during boreal spring (MAM; Fig. 4), when the double ITCZ bias is also the most prominent, and weakest during boreal fall (SON; Fig. S4), with summer and winter (JJA and DJF) exhibiting responses between the other two seasons. The northward ITCZ shift is associated with a southerly wind anomaly just south of the equator that weakens the prevailing northeasterly winds and increases SSTs in this region (Wallace et al., 1989; Mitchell & Wallace, 1992) (Fig. 2e-j, Fig. S2e-j)—a positive feedback that contributes to the reduced SST and precipitation biases in the eastern Pacific (Fig. 5, Fig. S4). Altogether, the seasonal and annual-mean double ITCZ bias seen in FLOR Control and CESM Control is substantially mitigated in FLOR HiTopo, FLOR CAM, and FLOR Ideal CAM, indicating that orographic height over Central America plays a key role in tropical eastern Pacific ocean and atmosphere circulation, SSTs, and ITCZ position in the present climate. Additionally, comparing FLOR HiTopo and FLOR CAM, Central American orography appears to contribute more to the East Pacific climate biases than the orography in other regions such as the Andes, which are thought to play a major role in shaping the climate of this region (Takahashi & Battisti, 2007).

GCMs with improved climatologies, achieved for example through flux-adjustment or improved process representation, generally exhibit improved ENSO characteristics (Vecchi et al., 2014; Krishnamurthy et al., 2015; Choi, 2015; Delworth et al., 2020). In line with this prior finding, we find that the raised orography simulations improve several aspects



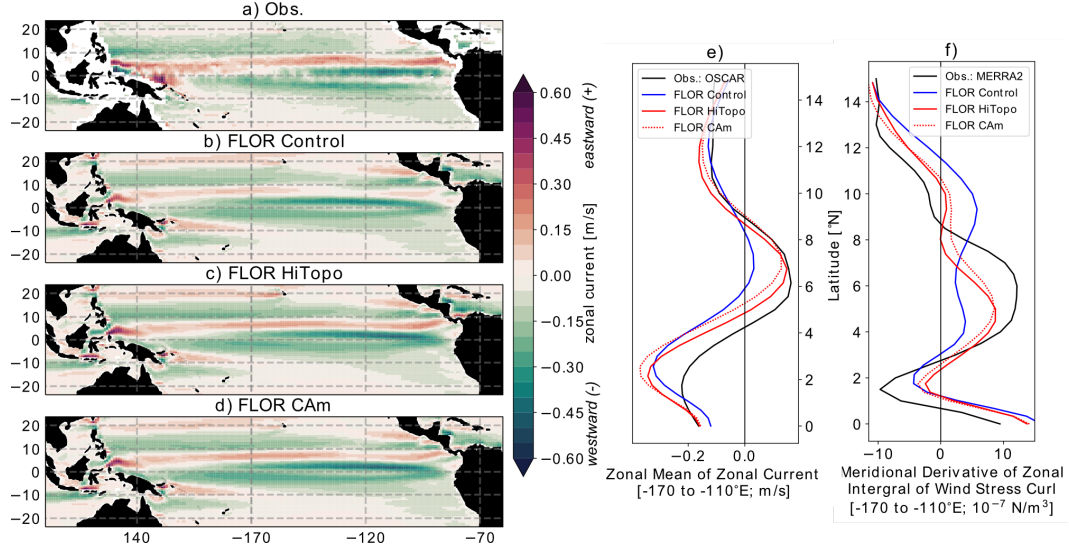


**Figure 3. Zonal currents and related winds in FLOR.** Time mean zonal currents across the tropical Pacific are shaded for observations (OSCAR; a), FLOR Control (b), FLOR HiTopo (c), and FLOR CAM (d). Before plotting, the OSCAR data ( $0.33^\circ \times 0.33^\circ$ ) is regridded to the FLOR ocean grid. To highlight and understand changes in the north equatorial counter current (NECC), zonal means of these zonal currents are plotted for the northern tropics (e), and compared to the meridional derivatives of the zonal integrals of wind stress curl (f); in (e) and (f) observations are plotted in black, FLOR Control is blue, FLOR HiTopo is red, and FLOR CAM is dashed red.

of the models' ENSO variability. Most notably, in the raised orography simulations of both FLOR and CESM, the amplitude of ENSO's seasonal cycle of variance (normalized by total variance) increases to be more in line with observations (Fig. 6). The phasing in the seasonality of ENSO is also somewhat improved when compared to observations, although in CESM the annual cycle in variance in both Control and Ideal CAM is shifted to later in the calendar year by around two months relative to observations. The overall magnitude of ENSO variance is also reduced to be more in line with observations in FLOR HiTopo and FLOR CAM compared to FLOR Control (interior barplots in Fig. 6a,b; and Fig. S6a,b). This improvement in magnitude is not seen in CESM Ideal CAM compared to CESM Control, though the magnitude of the variance bias is notably weaker in CESM Control than in FLOR Control (Fig. 6c,d, and Fig. S6c,d). Additionally, the low bias in Niño 3/3.4 SST anomaly skewness seen in both FLOR and CESM Controls does not improve with elevated orography (not shown). The ENSO simulated by FLOR HiTopo is more similar to that observed than FLOR CAM, suggesting that the Central American orography, Andes, and perhaps even further remote orography, all play roles in shaping ENSO.

Outside the tropical Pacific, the raised FLOR HiTopo orography leads to improvements elsewhere, including over land. GCMs including FLOR often exhibit wet biases in precipitation over western North America (Johnson et al., 2020; van der Wiel et al., 2016). While these precipitation biases are partially attributable to SST biases (Johnson et al., 2020), we find that the artificially low GCM orography also substantially contributes to these precipitation biases. In FLOR HiTopo compared to FLOR Control, the wet bias in western North America is significantly reduced, leading to a more accurate spatial distribution of precipitation (Fig. S5). These biases are partially connected to SST improve-

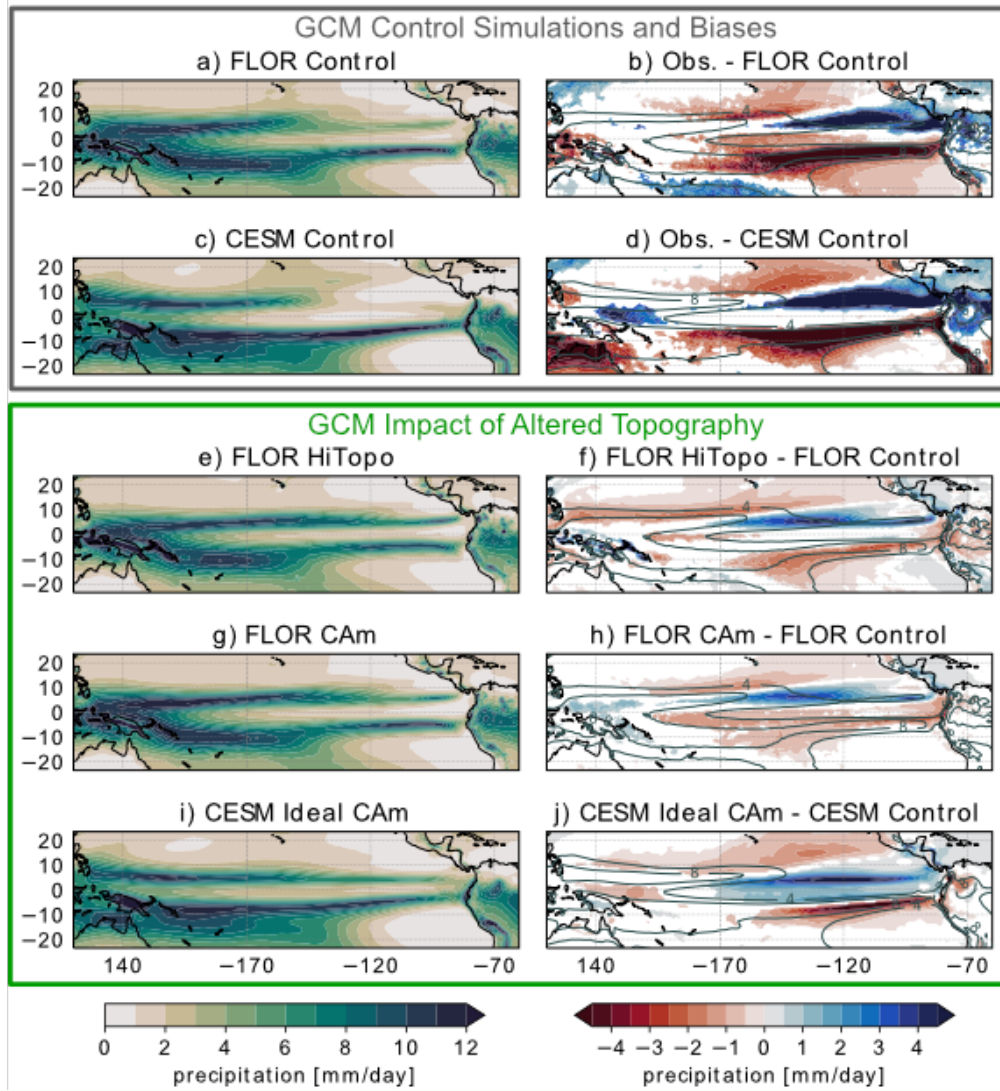


**Figure 4. Influence of high orography on precipitation in the tropical Pacific for MAM.** The left column shows MAM seasonal mean precipitation over the tropical Pacific for each of the model runs– FLOR Control (a), CESM Control (c), FLOR HiTopo (e), FLOR CAM (g), and CESM Ideal CAM (i). The right column shows differences between MAM seasonal mean precipitation for observations vs. Control simulations– Obs. vs. FLOR Control (b), Obs. vs. CESM Control (d)– and altered orography vs. Control simulations– FLOR HiTopo vs. FLOR Control (f), FLOR CAM vs. FLOR Control (h), CESM Ideal CAM vs. CESM Control (j). In these right column difference panels (b,d,f,h,j), the corresponding FLOR or CESM Control simulation MAM precipitation climatology is contoured in dark gray-green, with contour labels in mm/day. In the right panels, differences that are not significant at a 90% level based on a two-sided  $t$ -test are masked white.

ments that are also seen in the FLOR CAM experiment, but mainly arise due to orographic changes outside of Central America. There are a few possible reasons for this change, including higher Rocky Mountains presenting a more significant barrier for the Great Plains Low Level Jet and Pacific storm track, shifts in atmospheric wave patterns

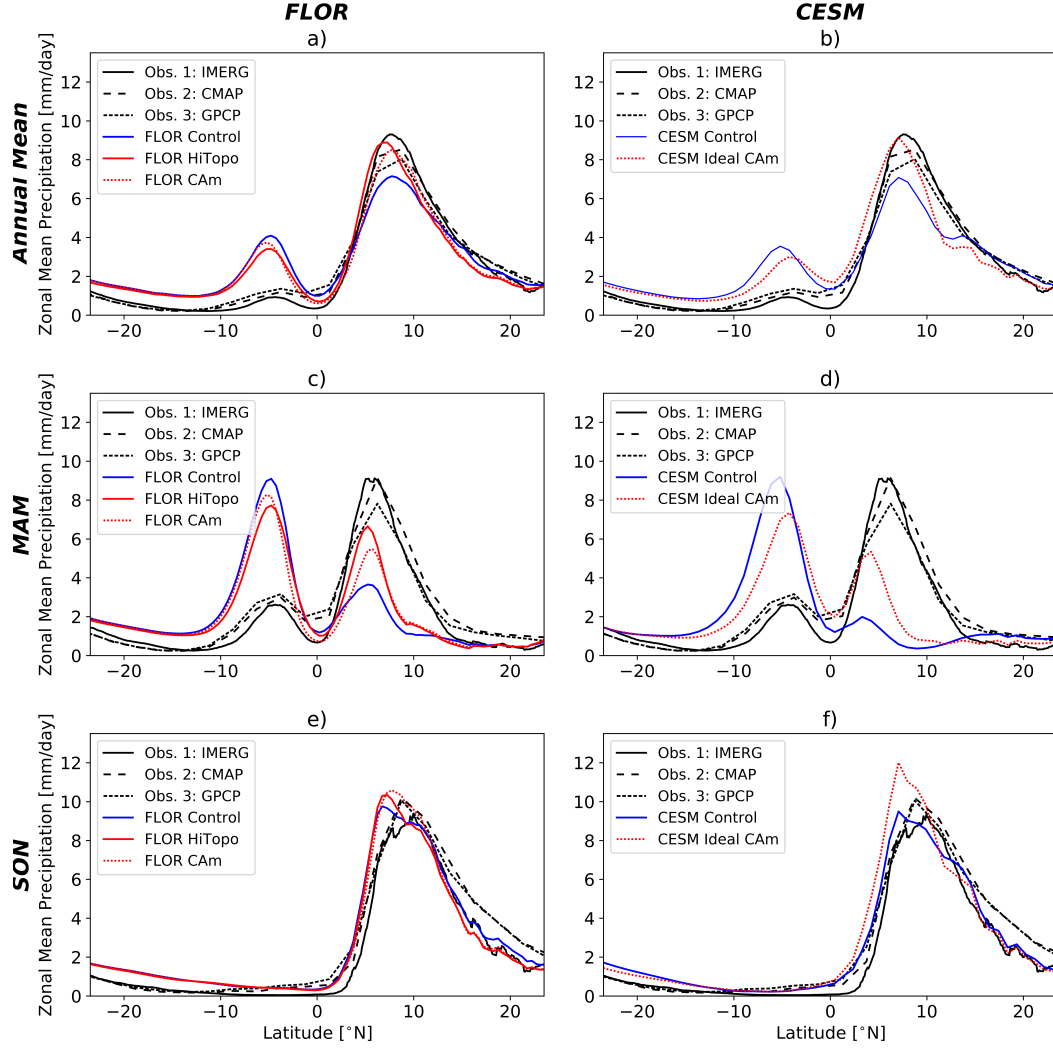


**Figure 5. Eastern tropical Pacific zonal mean precipitation.** Precipitation during MAM masked over the ocean and averaged over 130 to 75°W is plotted for the annual mean (a,b), MAM seasonal mean (c,d), and SON seasonal mean (e,f). In all panels, black lines plot three different gridded observations (IMERG in solid black, CMAP in wide black dashes, and GPCP in small black dashes). In the left column, the colored lines plot FLOR Control (blue), FLOR HiTopo (red), and FLOR CAm (dashed red). In the right column, the colored lines plot CESM Control (blue) and CESM Ideal CAm (dashed red).

or the westerly jet from elevated orography across the world, or more realistic ENSO teleconnections. We leave disentangling these dynamics to future work.

#### 4 Discussion & Conclusions

Altogether, these experiments provide strong evidence that orography plays a key role in shaping the climate of the tropical East Pacific, and that overly smoothed orography in GCMs leads to substantial biases in this region. Central American orography blocks the flow of easterlies into the northeastern tropical Pacific, warming this region through reduced air-sea fluxes and ocean upwelling and an enhanced NECC, which in

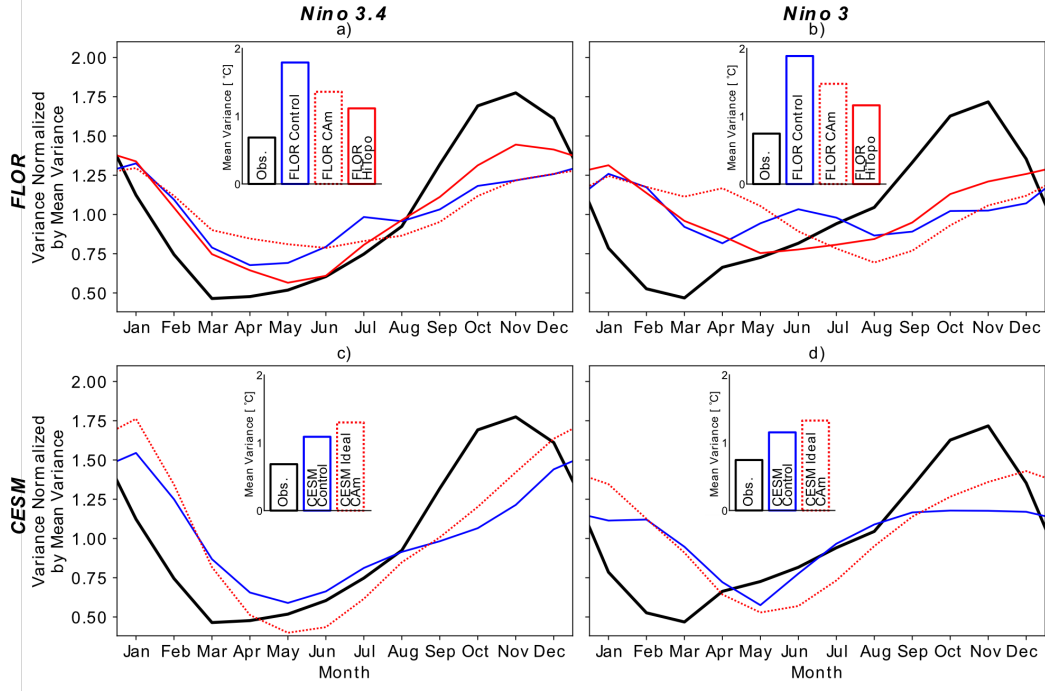


**Figure 6. Seasonal cycle of ENSO variance.** Variance of ENSO SST anomalies as a function of month normalized by annual mean variance (line plots) and the annual mean variance of ENSO SST anomalies (bar plots within each panel) are plotted for the Niño 3.4 index (left column), and the Niño 3 index (right column). In all panels HadISST observations are shown in black. In the top row, FLOR results are shown (FLOR Control is blue, FLOR CAM is dashed red, and FLOR HiTopo is solid red), while in the bottom row CESM results are shown (CESM Control is blue, CESM Ideal CAM is dashed red).

turn leads to enhanced precipitation. Insufficiently high orography in Central and South America leads the northeastern tropical Pacific to be biased cool and dry, with a weakened NECC, and the southeastern tropical Pacific to be biased wet (especially in the lower-resolution CESM), substantially enhancing the double ITCZ bias. Prior work has demonstrated that the Andes interact with the zonal flow to create subsidence of dry air to their west, which increases latent heat fluxes and cools the southeastern tropical Pacific, reducing precipitation there (Takahashi & Battisti, 2007). Comparing FLOR HiTopo and FLOR CAM results, elevating Central American orography plays a more influential role in reducing the biases in eastern Pacific climatology than does elevating the Andes.

The low orography present in GCMs also leads to biases in ENSO simulation. Both in CESM and in FLOR, increased orographic blocking causes greater seasonality in ENSO variance (Fig. 6) that is more in line with that observed, though biases still exist in the phasing of the seasonal cycle of variance (including a two-month phase shift in CESM relative to observations). This improvement likely due to a northward shift in the climatological precipitation centroid in the eastern Pacific in MAM (i.e. reduction in the double ITCZ bias), which results in an enhanced annual harmonic in the climatology of the equatorial atmosphere-ocean system in the deep tropics (and a reduction in the semi-annual harmonic (Giese & Carton, 1994)). A variety of mechanisms closely link the climatological seasonal cycle of atmosphere-ocean coupling to ENSO, as the seasonal cycle of atmosphere-ocean coupling forces Rossby and Kelvin waves which amplify and terminate ENSO events (Battisti, 1988; Thompson & Battisti, 2000, 2001). Additionally,

the termination of ENSO events has been tied to meridional shifts of westerly wind anomalies caused by seasonal movement of the warmest SSTs (Harrison & Vecchi, 1999; Vecchi & Harrison, 2003, 2006; Spencer, 2004; McGregor et al., 2013). Altogether, the low orographic peaks present in GCMs likely bias ENSO by enhancing tropical Pacific mean state biases.

When a GCM is developed, the model parameters are tuned to generate the most accurate possible simulation of climate given the model structure. Because FLOR and CESM were optimized around their Control orography, the notable improvements in tropical climatology and variability are striking in the raised orography experiments, as they occur without any effort to re-tune the GCMs. We expect that even greater improvements could be possible if a GCM was developed and tuned with the raised orography.

These results suggest a logical pathway for reducing tropical biases in climate models, starting with a physically-based change in how orography is prescribed in the models to better retain mountain peak heights. Our results show that this change in isolation can significantly affect major, long-standing biases in the simulated tropical climatology and interannual variability. The development of subgridscale parameterizations (such as clouds and subgridscale boundary layer processes in the atmosphere and ocean) would likely benefit if performed within models with a more realistic representation of the effective height of mountains. Additionally, experiments altering Central American orography in the lower resolution CESM suggest that HiTopo-style orographic boundary conditions can improve GCMs with a range of spatial resolutions. Alternative interpolations to better retain orographic height may be beneficial for a variety of studies using high-end climate models, including global warming simulations, seasonal forecasting, and more idealized experiments, such as those examining the climatic role of orography. Indeed, variations in orographic boundary conditions over Central America have already been shown to substantially alter the response of the ITCZ to North Atlantic meltwater forcing (Atwood et al., 2020).

In examining the large scales of atmospheric and oceanic circulation where GCMs excel, HiTopo confers numerous advantages to both the tropical mean climatology, its variability, and its teleconnections. However, it is important to note that HiTopo orography should not be expected to lead to a more realistic climate simulation in all regards. In particular, HiTopo orography could lead to degradation in the representation of very local climate effects around orography, by creating overly broad regions at mountain peak elevation and some unrealistically steep mountain slopes. Further, HiTopo orography should not be expected to correct biases that have a different root cause, such as inaccurate clouds or ocean mixing. Future work should explore optimal interpolation of orography onto the model grid to better capture the underestimated mechanical blocking effects of orography and minimize biases in simulated climate.

## Acknowledgments

This work is supported in part by NOAA/OCO (award NA18OAR4310418), NOAA/MAPP (award NA18OAR4310273), and the Carbon Mitigation Initiative (CMI) at Princeton University. J.W.B. was also funded by the Lamont-Doherty Earth Observatory Postdoctoral Fellowship. D.S.B. was funded by a gift from the Tamaki Foundation. Support was provided to A.R.A. by the National Science Foundation Paleo Perspective on Climate Change (P2C2) Grant AGS-1702827, and a fellowship from the National Oceanic and Atmospheric Administration Climate and Global Change Postdoctoral Program. We would like to acknowledge high-performance computing support from Cheyenne (doi:10.5065/D6RX99HX) provided by NCAR’s Computational and Information Systems Laboratory, sponsored by the National Science Foundation. The GFDL FLOR simulations were performed on computational resources managed and supported by Princeton Research Computing, a consortium of groups including the Princeton Institute for Computational Science and Engineering (PICSciE) and the Office of Information Technology’s High Performance Com-



puting Center and Visualization Laboratory at Princeton University. The source code for the GFDL CM2.5 (FLOR) is freely available at <https://www.gfdl.noaa.gov/cm2-5-and-flor>. Upon publication, model and observational data used in this paper’s analysis will be accessible at <http://tigress-web.princeton.edu/~janewb/HITOP0/>, and code to make the paper figures will be available at <https://github.com/janewbaldwin/HiTopo>. The authors declare that they have no competing financial interests.

## References

- Adler, R. F., Huffman, G. J., Chang, A., Ferraro, R., Xie, P.-P., Janowiak, J., ... others (2003). The version-2 global precipitation climatology project (GPCP) monthly precipitation analysis (1979-present). *Journal of Hydrometeorology*, 4(6), 1147–1167. Retrieved 2014-10-25, from [http://journals.ametsoc.org/doi/abs/10.1175/1525-7541\(2003\)004%3C1147:TVGPCP%3E2.0.CO;2](http://journals.ametsoc.org/doi/abs/10.1175/1525-7541(2003)004%3C1147:TVGPCP%3E2.0.CO;2)
- Atwood, A. R., Donohoe, A., Battisti, D. S., Liu, X., & Pausata, F. S. R. (2020). Robust Longitudinally Variable Responses of the ITCZ to a Myriad of Climate Forcings. *Geophysical Research Letters*, 47(17), e2020GL088833. Retrieved 2020-10-30, from <https://agupubs.onlinelibrary.wiley.com/doi/abs/10.1029/2020GL088833> (eprint: <https://agupubs.onlinelibrary.wiley.com/doi/pdf/10.1029/2020GL088833>) doi: 10.1029/2020GL088833
- Battisti, D. S. (1988, October). Dynamics and Thermodynamics of a Warming Event in a Coupled Tropical Atmosphere–Ocean Model. *Journal of the Atmospheric Sciences*, 45(20), 2889–2919. Retrieved 2020-08-05, from <https://journals.ametsoc.org/jas/article/45/20/2889/22178/Dynamics-and-Thermodynamics-of-a-Warming-Event-in> (Publisher: American Meteorological Society) doi: 10.1175/1520-0469(1988)045<2889:DATOAW>2.0.CO;2
- Bonjean, F., & Lagerloef, G. S. (2002). Diagnostic model and analysis of the surface currents in the tropical Pacific Ocean. *Journal of Physical Oceanography*, 32(10), 2938–2954.
- Boos, W. R., & Kuang, Z. (2010). Dominant control of the South Asian monsoon by orographic insulation versus plateau heating. *Nature*, 463(7278), 218–222. Retrieved 2013-05-24, from <http://www.nature.com/nature/journal/v463/n7278/abs/nature08707.html>
- Chiang, J. C. H., Fung, I. Y., Wu, C.-H., Cai, Y., Edman, J. P., Liu, Y., ... Labrousse, C. A. (2015, January). Role of seasonal transitions and westerly jets in East Asian paleoclimate. *Quaternary Science Reviews*, 108, 111–129. Retrieved 2015-06-21, from <http://www.sciencedirect.com/science/article/pii/S0277379114004570> doi: 10.1016/j.quascirev.2014.11.009
- Choi, K. Y. (2015). *El Niño–Southern Oscillation: Asymmetry, nonlinear atmospheric response and the role of mean climate* (PhD Thesis). Princeton University.
- Delworth, T. L., Cooke, W. F., Adcroft, A., Bushuk, M., Chen, J.-H., Dunne, K. A., ... Zhao, M. (2020). SPEAR: The Next Generation GFDL Modeling System for Seasonal to Multidecadal Prediction and Projection. *Journal of Advances in Modeling Earth Systems*, 12(3), e2019MS001895. Retrieved 2020-08-24, from <https://agupubs.onlinelibrary.wiley.com/doi/abs/10.1029/2019MS001895> (eprint: <https://agupubs.onlinelibrary.wiley.com/doi/pdf/10.1029/2019MS001895>) doi: 10.1029/2019MS001895
- Fu, D., Chang, P., & Patricola, C. M. (2017, May). Intrabasin Variability of East Pacific Tropical Cyclones During ENSO Regulated by Central American Gap Winds. *Scientific Reports*, 7(1), 1658. Retrieved 2020-09-09, from <https://www.nature.com/articles/s41598-017-01962-3> (Number: 1

- Publisher: Nature Publishing Group) doi: 10.1038/s41598-017-01962-3
- Gelaro, R., McCarty, W., Suárez, M. J., Todling, R., Molod, A., Takacs, L., ... Reichle, R. (2017). The modern-era retrospective analysis for research and applications, version 2 (MERRA-2). *Journal of Climate*, 30(14), 5419–5454.
- Giese, B. S., & Carton, J. A. (1994, August). The Seasonal Cycle in Coupled Ocean-Atmosphere Model. *Journal of Climate*, 7(8), 1208–1217. Retrieved 2020-08-05, from <https://journals.ametsoc.org/jcli/article/7/8/1208/35582/The-Seasonal-Cycle-in-Coupled-Ocean-Atmosphere> (Publisher: American Meteorological Society) doi: 10.1175/1520-0442(1994)007<1208:TSCICO>2.0.CO;2
- Harrison, D. E., & Vecchi, G. A. (1999). On the termination of El Niño. *Geophysical Research Letters*, 26(11), 1593–1596. Retrieved 2020-05-08, from <https://agupubs.onlinelibrary.wiley.com/doi/abs/10.1029/1999GL900316> (eprint: <https://agupubs.onlinelibrary.wiley.com/doi/pdf/10.1029/1999GL900316>) doi: 10.1029/1999GL900316
- Holton, J. R. (1973). An introduction to dynamic meteorology. *American Journal of Physics*, 41(5), 752–754. (Publisher: American Association of Physics Teachers)
- Hoskins, B. J., & Karoly, D. J. (1981). The steady linear response of a spherical atmosphere to thermal and orographic forcing. *Journal of the Atmospheric Sciences*, 38(6), 1179–1196. Retrieved 2013-12-16, from [http://journals.ametsoc.org/doi/abs/10.1175/1520-0469\(1981\)038%3C1179%3ATSRLROA%3E2.0.CO%3B2](http://journals.ametsoc.org/doi/abs/10.1175/1520-0469(1981)038%3C1179%3ATSRLROA%3E2.0.CO%3B2)
- Huffman, G., Bolvin, D., Braithwaite, D., Hsu, K., Joyce, R., & Xie, P. (n.d.). *Integrated multi-satellite retrievals for GPM (IMERG), version 4.4*. NASA's Precipitation Processing Center.
- Jarraud, M., Simmons, A., & Kanamitsu, M. (1986). *The concept, implementation and impact of an envelope orography*. (Pages: 81-128 Place: Shinfield Park, Reading Publisher: ECMWF Volume: 2)
- Jia, L., Vecchi, G. A., Yang, X., Gudgel, R. G., Delworth, T. L., Stern, W. F., ... Zeng, F. (2016). The roles of radiative forcing, sea surface temperatures, and atmospheric and land initial conditions in US summer warming episodes. *Journal of Climate*, 29(11), 4121–4135. Retrieved 2017-05-13, from <http://journals.ametsoc.org/doi/abs/10.1175/JCLI-D-15-0471.1>
- Jia, L., Yang, X., Vecchi, G. A., Gudgel, R. G., Delworth, T. L., Rosati, A., ... Dixon, K. (2014, December). Improved Seasonal Prediction of Temperature and Precipitation over Land in a High-Resolution GFDL Climate Model. *Journal of Climate*, 28(5), 2044–2062. Retrieved 2018-06-01, from <https://journals.ametsoc.org/doi/10.1175/JCLI-D-14-00112.1> doi: 10.1175/JCLI-D-14-00112.1
- Johnson, N. C., Krishnamurthy, L., Wittenberg, A. T., Xiang, B., Vecchi, G. A., Kapnick, S., & Pascale, S. (2020, January). The impact of sea surface temperature biases on North American precipitation in a high-resolution climate model. *Journal of Climate*. Retrieved 2020-02-19, from <https://journals.ametsoc.org/doi/abs/10.1175/JCLI-D-19-0417.1> doi: 10.1175/JCLI-D-19-0417.1
- Kessler, W. S. (2006, May). The circulation of the eastern tropical Pacific: A review. *Progress in Oceanography*, 69(2), 181–217. Retrieved 2019-03-20, from <http://www.sciencedirect.com/science/article/pii/S00796661106000310> doi: 10.1016/j.pocean.2006.03.009
- Kong, W., & Chiang, J. C. (2020). Interaction of the westerlies with the Tibetan Plateau in determining the mei-yu termination. *Journal of Climate*, 33(1), 339–363.
- Krishnamurthy, L., Vecchi, G. A., Msadek, R., Wittenberg, A., Delworth, T. L., &

- Zeng, F. (2015, June). The Seasonality of the Great Plains Low-Level Jet and ENSO Relationship. *Journal of Climate*, 28(11), 4525–4544. Retrieved 2020-08-05, from <https://journals.ametsoc.org/jcli/article/28/11/4525/34306/The-Seasonality-of-the-Great-Plains-Low-Level-Jet> (Publisher: American Meteorological Society) doi: 10.1175/JCLI-D-14-00590.1
- Krishnamurthy, L., Vecchi, G. A., Yang, X., van der Wiel, K., Balaji, V., Kaplan, S. B., ... Underwood, S. (2018, February). Causes and probability of occurrence of extreme precipitation events like Chennai 2015. *Journal of Climate*. Retrieved 2018-03-31, from <https://journals.ametsoc.org/doi/abs/10.1175/JCLI-D-17-0302.1> doi: 10.1175/JCLI-D-17-0302.1
- McGregor, S., Ramesh, N., Spence, P., England, M. H., McPhaden, M. J., & Santoso, A. (2013). Meridional movement of wind anomalies during ENSO events and their role in event termination. *Geophysical Research Letters*, 40(4), 749–754. Retrieved 2020-05-08, from <https://agupubs.onlinelibrary.wiley.com/doi/abs/10.1002/grl.50136> (eprint: <https://agupubs.onlinelibrary.wiley.com/doi/pdf/10.1002/grl.50136>) doi: 10.1002/grl.50136
- Mitchell, T. P., & Wallace, J. M. (1992, October). The Annual Cycle in Equatorial Convection and Sea Surface Temperature. *Journal of Climate*, 5(10), 1140–1156. Retrieved 2020-08-05, from <https://journals.ametsoc.org/jcli/article/5/10/1140/35414/The-Annual-Cycle-in-Equatorial-Convection-and-Sea> (Publisher: American Meteorological Society) doi: 10.1175/1520-0442(1992)005<1140:TACIEC>2.0.CO;2
- Molnar, P., Boos, W. R., & Battisti, D. S. (2010). Orographic controls on climate and paleoclimate of Asia: thermal and mechanical roles for the Tibetan Plateau. *Annual Review of Earth and Planetary Sciences*, 38(1), 77. Retrieved 2014-02-21, from <http://www.annualreviews.org/eprint/zkgB9iicZa3YKrg3cemj/full/10.1146/annurev-earth-040809-152456>
- Oueslati, B., & Bellon, G. (2015). The double ITCZ bias in CMIP5 models: interaction between SST, large-scale circulation and precipitation. *Climate dynamics*, 44(3-4), 585–607. (Publisher: Springer)
- Putman, W. M., & Lin, S.-J. (2007). Finite-volume transport on various cubed-sphere grids. *Journal of Computational Physics*, 227(1), 55–78. (Publisher: Elsevier)
- Rayner, N. A., Parker, D. E., Horton, E. B., Folland, C. K., Alexander, L. V., Rowell, D. P., ... Kaplan, A. (2003). Global analyses of sea surface temperature, sea ice, and night marine air temperature since the late nineteenth century. *Journal of Geophysical Research: Atmospheres*, 108(D14). Retrieved 2017-02-02, from <http://onlinelibrary.wiley.com/doi/10.1029/2002JD002670/full>
- Reid, R. O. (1948). The equatorial currents of the eastern Pacific as maintained by the stress of the wind. *Journal of Marine Research*, 7(2), 74–99. (Publisher: KLINE GEOLOGY LABORATORY YALE UNIV, NEW HAVEN, CT 06520-8109)
- Shi, Z., Sha, Y., & Liu, X. (2016, November). Effect of Yunnan–Guizhou Topography at the Southeastern Tibetan Plateau on the Indian Monsoon. *Journal of Climate*, 30(4), 1259–1272. Retrieved 2020-04-06, from <https://journals.ametsoc.org/doi/full/10.1175/JCLI-D-16-0105.1> (Publisher: American Meteorological Society) doi: 10.1175/JCLI-D-16-0105.1
- Song, F., & Zhang, G. J. (2020, February). The Impacts of Horizontal Resolution on the Seasonally Dependent Biases of the Northeastern Pacific ITCZ in Coupled Climate Models. *Journal of Climate*, 33(3), 941–957. Retrieved 2020-09-11, from <https://journals.ametsoc.org/jcli/article/33/3/941/346248/The-Impacts-of-Horizontal-Resolution-on-the> (Publisher: American Meteorological Society) doi: 10.1175/JCLI-D-19-0399.1

- 555 Spencer, H. (2004). Role of the atmosphere in seasonal phase lock-  
 556 ing of El Niño. *Geophysical Research Letters*, 31(24). Re-  
 557 trieved 2020-05-08, from [https://agupubs.onlinelibrary](https://agupubs.onlinelibrary.wiley.com/doi/abs/10.1029/2004GL021619)  
 558 [.wiley.com/doi/abs/10.1029/2004GL021619](https://agupubs.onlinelibrary.wiley.com/doi/abs/10.1029/2004GL021619) (\_eprint:  
 559 <https://agupubs.onlinelibrary.wiley.com/doi/pdf/10.1029/2004GL021619>)  
 560 doi: 10.1029/2004GL021619
- 561 Steenburgh, W. J., Schultz, D. M., & Colle, B. A. (1998, October). The Struc-  
 562 ture and Evolution of Gap Outflow over the Gulf of Tehuantepec, Mexico.  
 563 *Monthly Weather Review*, 126(10), 2673–2691. Retrieved 2018-02-23, from  
 564 [https://journals.ametsoc.org/doi/abs/10.1175/1520-0493\(1998\)126%](https://journals.ametsoc.org/doi/abs/10.1175/1520-0493(1998)126%3C2673:TSAEOG%3E2.0.CO%3B2)  
 565 [3C2673:TSAEOG%3E2.0.CO%3B2](https://journals.ametsoc.org/doi/abs/10.1175/1520-0493(1998)126%3C2673:TSAEOG%3E2.0.CO%3B2) doi: 10.1175/1520-0493(1998)126(2673:  
 566 TSAEOG)2.0.CO;2
- 567 Sun, F., & Yu, J.-Y. (2006). Impacts of Central America gap winds on the  
 568 SST annual cycle in the eastern Pacific warm pool. *Geophysical Re-*  
 569 *search Letters*, 33(6). Retrieved 2020-03-23, from [https://agupubs](https://agupubs.onlinelibrary.wiley.com/doi/abs/10.1029/2005GL024700)  
 570 [.onlinelibrary.wiley.com/doi/abs/10.1029/2005GL024700](https://agupubs.onlinelibrary.wiley.com/doi/abs/10.1029/2005GL024700) (\_eprint:  
 571 <https://agupubs.onlinelibrary.wiley.com/doi/pdf/10.1029/2005GL024700>) doi:  
 572 10.1029/2005GL024700
- 573 Sverdrup, H. U. (1947, November). Wind-Driven Currents in a Baroclinic Ocean;  
 574 with Application to the Equatorial Currents of the Eastern Pacific. *Proceedings*  
 575 *of the National Academy of Sciences of the United States of America*, 33(11),  
 576 318–326. Retrieved 2020-08-05, from [https://www.ncbi.nlm.nih.gov/pmc/](https://www.ncbi.nlm.nih.gov/pmc/articles/PMC1079064/)  
 577 [articles/PMC1079064/](https://www.ncbi.nlm.nih.gov/pmc/articles/PMC1079064/)
- 578 Takahashi, K., & Battisti, D. S. (2007). Processes controlling the mean tropical  
 579 Pacific precipitation pattern. Part II: The SPCZ and the southeast Pacific dry  
 580 zone. *Journal of Climate*, 20(23), 5696–5706. Retrieved 2017-01-19, from  
 581 <http://journals.ametsoc.org/doi/abs/10.1175/2007JCLI1656.1>
- 582 Thompson, C. J., & Battisti, D. S. (2000, August). A Linear Stochastic Dynamical  
 583 Model of ENSO. Part I: Model Development. *Journal of Climate*, 13(15),  
 584 2818–2832. Retrieved 2020-08-05, from [https://journals.ametsoc.org/](https://journals.ametsoc.org/jcli/article/13/15/2818/105291/A-Linear-Stochastic-Dynamical-Model-of-ENSO-Part-I)  
 585 [jcli/article/13/15/2818/105291/A-Linear-Stochastic-Dynamical](https://journals.ametsoc.org/jcli/article/13/15/2818/105291/A-Linear-Stochastic-Dynamical-Model-of-ENSO-Part-I)  
 586 [-Model-of-ENSO-Part-I](https://journals.ametsoc.org/jcli/article/13/15/2818/105291/A-Linear-Stochastic-Dynamical-Model-of-ENSO-Part-I) (Publisher: American Meteorological Society)  
 587 doi: 10.1175/1520-0442(2000)013(2818:ALSDMO)2.0.CO;2
- 588 Thompson, C. J., & Battisti, D. S. (2001). A linear stochastic dynamical model of  
 589 ENSO. Part II: Analysis. *Journal of Climate*, 14(4), 445–466.
- 590 Valdes, P. J., & Hoskins, B. J. (1991). Nonlinear orographically forced planetary  
 591 waves. *Journal of the atmospheric sciences*, 48(18), 2089–2106.
- 592 van der Wiel, K., Kapnick, S. B., Vecchi, G. A., Cooke, W. F., Delworth, T. L., Jia,  
 593 L., ... Zeng, F. (2016). The resolution dependence of contiguous U.S. pre-  
 594 cipitation extremes in response to CO2 forcing. *Journal of Climate*, 29(22),  
 595 7991–8012. Retrieved 2017-02-01, from [http://journals.ametsoc.org/doi/](http://journals.ametsoc.org/doi/abs/10.1175/JCLI-D-16-0307.1)  
 596 [abs/10.1175/JCLI-D-16-0307.1](http://journals.ametsoc.org/doi/abs/10.1175/JCLI-D-16-0307.1)
- 597 Vecchi, G. A., Delworth, T., Gudgel, R., Kapnick, S., Rosati, A., Wittenberg, A. T.,  
 598 ... Zhang, S. (2014, July). On the Seasonal Forecasting of Regional Tropical  
 599 Cyclone Activity. *Journal of Climate*, 27(21), 7994–8016. Retrieved from  
 600 <http://journals.ametsoc.org/doi/abs/10.1175/JCLI-D-14-00158.1> doi:  
 601 10.1175/JCLI-D-14-00158.1
- 602 Vecchi, G. A., & Harrison, D. E. (2003). On the termination of the  
 603 2002–03 El Niño event. *Geophysical Research Letters*, 30(18).  
 604 Retrieved 2020-05-08, from [https://agupubs.onlinelibrary](https://agupubs.onlinelibrary.wiley.com/doi/abs/10.1029/2003GL017564)  
 605 [.wiley.com/doi/abs/10.1029/2003GL017564](https://agupubs.onlinelibrary.wiley.com/doi/abs/10.1029/2003GL017564) (\_eprint:  
 606 <https://agupubs.onlinelibrary.wiley.com/doi/pdf/10.1029/2003GL017564>)  
 607 doi: 10.1029/2003GL017564
- 608 Vecchi, G. A., & Harrison, D. E. (2006, June). The Termination of the 1997–98  
 609 El Niño. Part I: Mechanisms of Oceanic Change. *Journal of Climate*, 19(12),

- 2633–2646. Retrieved 2020-05-08, from <https://journals.ametsoc.org/doi/full/10.1175/JCLI3776.1> (Publisher: American Meteorological Society) doi: 10.1175/JCLI3776.1
- Wallace, J. M., Mitchell, T. P., & Deser, C. (1989, December). The Influence of Sea-Surface Temperature on Surface Wind in the Eastern Equatorial Pacific: Seasonal and Interannual Variability. *Journal of Climate*, 2(12), 1492–1499. Retrieved 2020-08-05, from <https://journals.ametsoc.org/jcli/article/2/12/1492/31409/The-Influence-of-Sea-Surface-Temperature-on> (Publisher: American Meteorological Society) doi: 10.1175/1520-0442(1989)002<1492:TIOSST>2.0.CO;2
- Wallace, J. M., Tibaldi, S., & Simmons, A. J. (1983). Reduction of systematic forecast errors in the ECMWF model through the introduction of an envelope orography. *Quarterly Journal of the Royal Meteorological Society*, 109(462), 683–717. Retrieved 2020-08-24, from <https://rmets.onlinelibrary.wiley.com/doi/abs/10.1002/qj.49710946202> (eprint: <https://rmets.onlinelibrary.wiley.com/doi/pdf/10.1002/qj.49710946202>) doi: 10.1002/qj.49710946202
- White, R. H., Battisti, D. S., & Roe, G. H. (2017). Mongolian Mountains Matter Most: Impacts of the Latitude and Height of Asian Orography on Pacific Wintertime Atmospheric Circulation. *Journal of Climate*, 30(2017). Retrieved 2017-04-18, from <http://journals.ametsoc.org/doi/abs/10.1175/JCLI-D-16-0401.1>
- Xie, P., & Arkin, P. A. (1997). Global precipitation: A 17-year monthly analysis based on gauge observations, satellite estimates, and numerical model outputs. *Bulletin of the American Meteorological Society*, 78(11), 2539–2558. Retrieved 2014-10-25, from [http://journals.ametsoc.org/doi/abs/10.1175/1520-0477\(1997\)078%3C2539:GPAYMA%3E2.0.CO;2](http://journals.ametsoc.org/doi/abs/10.1175/1520-0477(1997)078%3C2539:GPAYMA%3E2.0.CO;2)
- Xie, S.-P., Xu, H., Kessler, W. S., & Nonaka, M. (2005). Air–sea interaction over the eastern Pacific warm pool: Gap winds, thermocline dome, and atmospheric convection. *Journal of Climate*, 18(1), 5–20.
- Xu, W. (2019). How South American Topography Influences Climate Simulation over the South Pacific Ocean in CESM. In *AGU Fall Meeting 2019*. AGU.